OPEN ACCESS Freely available online

PLOS ONE

Isocitrate Dehydrogenase from *Streptococcus mutans*: Biochemical Properties and Evaluation of a Putative Phosphorylation Site at Ser102

Peng Wang, Ping Song, Mingming Jin, Guoping Zhu*

Key Laboratory of Molecular Evolution and Biodiversity and Institute of Molecular Biology and Biotechnology, College of Life Sciences, Anhui Normal University, Wuhu, Anhui, China

Abstract

Isocitrate deyhdrogenase (IDH) is a reversible enzyme in the tricarboxylic acid cycle that catalyzes the NAD(P)$^+$-dependent oxidative decarboxylation of isocitrate to α-ketoglutarate (αKG) and the NAD(P)H/CO_2-dependent reductive carboxylation of αKG to isocitrate. The IDH gene from *Streptococcus mutans* was fused with the *icd* gene promoter from *Escherichia coli* to initiate its expression in the glutamate auxotrophic strain *E. coli ΔicdA::kan*^{r} of which the *icd* gene has been replaced by kanamycin resistance gene. The expression of *S. mutans* IDH (SmIDH) may restore the wild-type phenotype of the *icd*-defective strain on minimal medium without glutamate. The molecular weight of SmIDH was estimated to be 70 kDa by gel filtration chromatography, suggesting a homodimeric structure. SmIDH was divalent cation-dependent and Mn^{2+} was found to be the most effective cation. The optimal pH of SmIDH was 7.8 and the maximum activity was around 45°C. SmIDH was completely NAD^+ dependent and its apparent K_m for NAD^+ was 137 μM. In order to evaluate the role of the putative phosphorylation site at Ser102 in catalysis, two ''stably phosphorylated'' mutants were constructed by converting Ser102 into Glu102 or Asp102 in SmIDH to mimick a constitutively phosphorylated state. Meanwhile, the functional roles of another four amino acids (threonine, glycine, alanine and tyrosine) containing variant size of side chains were investigated. The replacement of Asp102 or Glu102 totally inactivated the enzyme, while the S102T, S102G, S102A and S102Y mutants decreased the affinity to isocitrate and only retained 16.0%, 2.8%, 3.3% and 1.1% of the original activity, respectively. These results reveal that Ser102 plays important role in substrate binding and is required for the enzyme function. Also, Ser102 in SmIDH is a potential phosphorylation site, indicating that the ancient NAD-dependent IDHs might be the underlying origin of ''phosphorylation mechanism'' used by their bacterial NADP-dependent homologs.

Citation: Wang P, Song P, Jin M, Zhu G (2013) Isocitrate Dehydrogenase from *Streptococcus mutans*: Biochemical Properties and Evaluation of a Putative Phosphorylation Site at Ser102. PLoS ONE 8(3): e58918. doi:10.1371/journal.pone.0058918

Editor: Roman Tuma, University of Leeds, United Kingdom

Received October 9, 2012; **Accepted** February 8, 2013; **Published** March 6, 2013

Copyright: © 2013 Wang et al. This is an open-access article distributed under the terms of the Creative Commons Attribution License, which permits unrestricted use, distribution, and reproduction in any medium, provided the original author and source are credited.

Funding: This research was supported by the National High Technology Research and Development Program (''863'' Program: 2012AA02A708), the National Natural Science Foundation of China (31170005; 30870062), Specialized Research Fund for the Doctoral Program of Higher Education of China (20113424110004), and the Fund of State Key Laboratory of Genetics Resources and Evolution from Kunming Institute of Zoology (CAS) (GREKF11-07). The funders had no role in study design, data collection and analysis, decision to publish, or preparation of the manuscript.

Competing Interests: The authors have declared that no competing interests exist.

* E-mail: gpz1996@yahoo.com

Introduction

Isocitrate deyhdrogenase (IDH) catalyzes the NAD(P)$^+$-dependent oxidative decarboxylation of isocitrate to α-ketoglutarate (αKG) and the NAD(P)H/CO_2- dependent reductive carboxylation of αKG to isocitrate using NAD^+ (EC 1.1.1.41) or $NADP^+$ (EC 1.1.1.42) as a cofactor. Phylogenetic analysis reveals that NAD^+ use by IDH is an ancestral phenotype and $NADP^+$ use by prokaryotic IDH arose on or about the time that eukaryotic mitochondria first appeared, some 3.5 billion years ago, in order to synthesize NADPH for bacterial adaptation on acetate [1]. As a better phenotype acquired through evolution, most IDHs exhibit the $NADP^+$ dependence, causing NAD^+ dependence comparatively uncommon among the bacterial IDHs. A small number of NAD^+-IDHs have been characterized in some bacteria and archaea [2–7]. A general feature shared by these organisms is that they have an incomplete tricarboxylic acid (TCA) cycle due to the absence of one or more TCA cycle enzymes [3]. Thus, these NAD^+-IDHs have been proposed to be reminiscent of the enzyme that participates in CO_2 fixation as well as glutamate biosynthesis [2,8]. Eukaryotic NAD^+-IDHs localize exclusively in the mitochondria and play a central catabolic role in energy production. The enzyme is structural complex and is rate-limiting in the TCA cycle as its affinity for substrate is allosterically regulated by ADP [9].

Eukaryotes have several types of $NADP^+$-dependent IDH isoenzymes, distributed in mitochondrial matrix, cell cytosol and peroxisome, respectively [10,11]. These enzymes share low sequence identity with prokaryotic counterparts, typified by $NADP^+$-IDH from *Escherichia coli* (EcIDH). Eukaryotic $NADP^+$-IDHs constitute a single clade in the phylogenetic tree, suggesting that they have evolved independently [5]. Mitochondrial isoenzymes provide auxiliary source of α-ketoglutarate and mitochondrial NADPH while the other two isoenzymes function in cellular defense against oxidative damage, detoxification of reactive oxygen species, and providing reducing power and carbon skeleton for fatty acids and amino acids biosynthesis [12–15]. Human cytosolic $NADP^+$-IDH1 has recently been reported to

be involved in tumorigenesis [16–18]. The IDH1 Arg132 mutation impairs the oxidative IDH activity of the enzyme, but acquires a new reduction function of converting α-ketoglutarate to 2-hydroxyglutarate, the resulting 2-hydroxyglutarate accumulation then induces the formation and malignant progression of tumors [19,20].

The prokaryotic $NADP^+$-IDHs have been extensively studied. EcIDH lies at the critical juncture between TCA cycle and the glyoxylate bypass, a pathway needed for growth on non-fermentative carbon sources such as acetate and ethanol. Under these stressful conditions, ~75% of EcIDH is completely inactivated by phosphorylation at Ser113 catalyzed by the bifunctional IDH kinase/phosphatase (IDH K/P), thereby partitioning most of the isocitrate through the glyoxylate shunt [21]. Briefly, isocitrate is hydrogen-bonded to the γ-hydroxyl of Ser113 in the active, dephosphorylated enzyme. The transfer of the γ-phosphate from ATP to Ser113 prevents isocitrate binding by eliminating this hydrogen bond and by introducing a source of electrostatic repulsion and steric hindrance with the γ-carboxylate of isocitrate [22–25]. This active serine in substrate binding is highly conserved in both prokaryotic and eukaryotic IDHs and the putative phosphorylation role of the equivalent serine in several $NADP^+$-IDHs have been discussed [10,11,26–28]. Although the $NADP^+$-IDH of *Bacillus subtilis* (BsIDH) is not regulated by phosphorylation *in vivo* due to the absence of the gene encoding IDH K/P in this organism, it serves as the substrate for *E. coli* IDH K/P *in vitro*, and the phosphorylation does occur at the expected serine and inhibits IDH activity [27]. Despite the high conservation of the analogous serine in NAD^+-IDHs, no studies have been reported yet to evaluate the possibility of the phosphorylation regulatory mechanism in these NAD^+-IDHs.

The NAD^+-dependent IDH of *S. mutans* (SmIDH) has a Ser102 at the position equivalent to Ser113 of EcIDH. In order to elucidate the function of Ser102, we generated two "stably phosphorylated" (pseudophosphorylated) mutants of SmIDH by converting Ser102 into glutamate or aspirate [29,30]. Meanwhile, another four mutations at site 102 were analyzed. These mutated enzymes were firstly screened by phenotypic complementation of *icd* deletion strain *E. coli* Δ*icd*::*kan*^{r} and then purified to homogeneity. The kinetic parameters of the wild-type together with the mutated enzymes were determined.

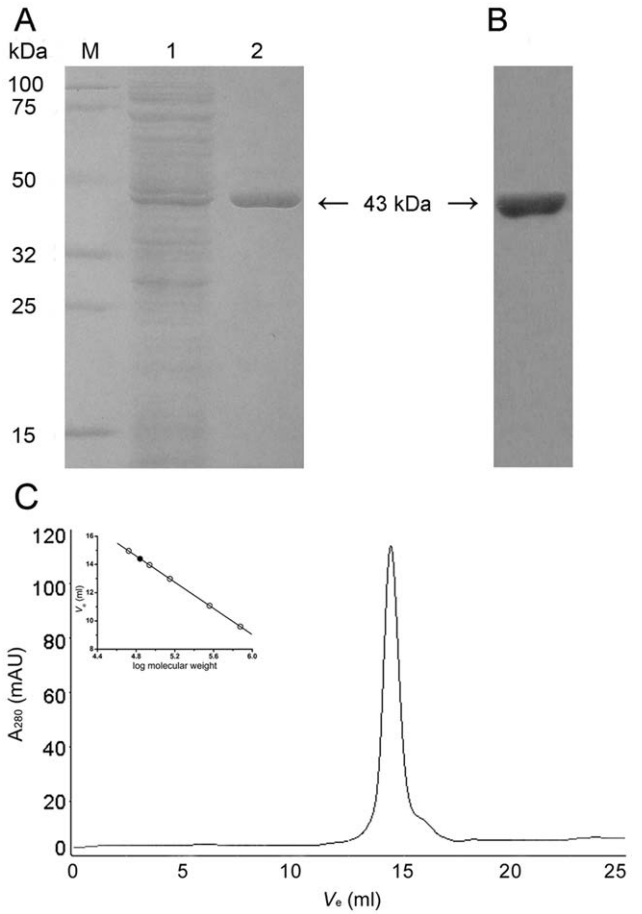

Figure 1. Enzyme purity, western blot and molecular mass analysis of SmIDH. (A) SDS-PAGE analysis of the expression and purification of SmIDH. Analysis was performed on 12% polyacrylamide gel. M, protein markers; lane 1, crude extracts of cells harboring pWT grown in MD medium without glutamate. lane 2, purified protein. (B) Western blot analysis using anti-6×His antibody as probe. (C) Molecular mass determination by gel filtration chromatography. The flow rate was 0.5 ml/min and the proteins in the fractions were monitored at 280 nm. Inside is the standard curve for molecular mass. SmIDH was represented as a dark circle (●). Standard proteins were represented by open circles (○): 1, Ovalbumin (44 kDa); 2, Conalbumin (75 kDa); 3, Aldolase (158 kDa); 4, Ferritin (440 kDa); 5, Thyroglobulin (669 kDa). V_e of SmIDH is 14.4 ml.
doi:10.1371/journal.pone.0058918.g001

Table 1. Construction of SmIDH mutants.

Enzyme	Amino acid sequence [a]	PCR	
		Template	Primer [b]
SmIDH	GIRSLNVALRQE		
S102T	- - - T - - - - - - - -	pWT	GGTATTCGTACTTTAAATGTTGCCCTGCGTCAAGAA
S102G	- - - G - - - - - - - -	pWT	GGTATTCGTGGCTTAAATGTTGCCCTGCGTCAAGAA
S102A	- - - A - - - - - - - -	pWT	GGTATTCGTGCTTTAAATGTTGCCCTGCGTCAAGAA
S102Y	- - - Y - - - - - - - -	pWT	GGTATTCGTTATTTAAATGTTGCCCTGCGTCAAGAA
S102D	- - - D - - - - - - - -	pWT	GGTATTCGTGATTTAAATGTTGCCCTGCGTCAAGAA
S102E	- - - E - - - - - - - -	pWT	GGTATTCGTGAATTAAATGTTGCCCTGCGTCAAGAA

[a]Dashes indicate the same amino acid residues as SmIDH.
[b]Only sense primers are shown. Underlines indicate mutated regions.
doi:10.1371/journal.pone.0058918.t001

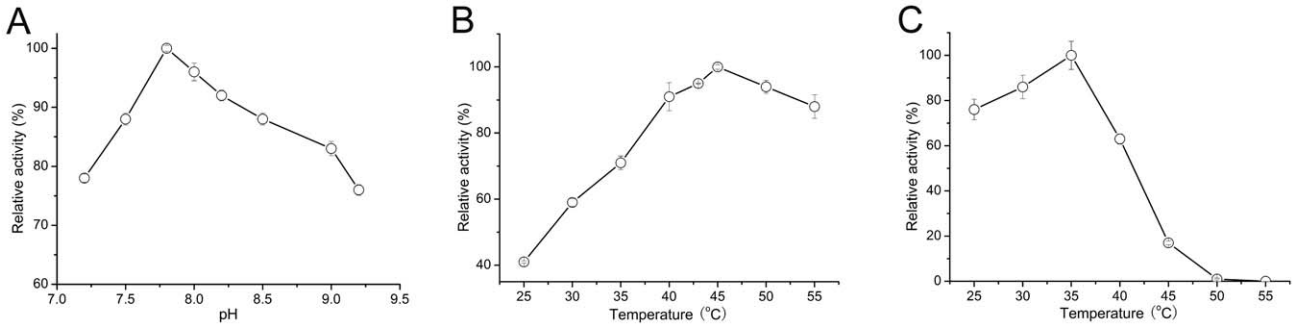

Figure 2. Effects of pH and temperature on the activity of purified SmIDH. (A) Effects of pH on SmIDH activity was measured with the pH range of 7.2–9.2. (B) Effects of temperature on SmIDH activity was measured from 25°C to 55°C. (C) Heat-inactivation profiles of SmIDH. The enzyme activity was measured from 25°C to 55°C.
doi:10.1371/journal.pone.0058918.g002

Materials and Methods

Strains, media and reagents

The *E. coli* strain *Δicd::kan*^{r} was presented by Antony M. Dean's laboratory (BioTechnology Institute, University of Minnesota, MN 55108, USA), which was constructed by replacing the entire *icd* cistron of *E. coli* strain CGSC6300 with a kanamycin cassette [1]. In our study, this auxotrophic strain was used as the host strain for the expression of SmIDH and its mutants. LB and MD media were prepared and supplemented with 100 μg/ml ampicillin and/or 30 μg/ml kanamycin as required. Plates contain 15 g/L agar. PrimeStar™ HS DNA polymerase was obtained from TaKaRa (Dalian, China). Restriction enzymes and protein molecular weight standards were purchased from Fermentas (Shanghai, China).

Plasmid construction

The 800-bp upstream region of the *icd* gene in the wildtype *E. coli* strain CGSC6300 was amplified with the following primers: *S-Ec*^{icdp}, 5′-atagatacctcgagCCATTGGCAAGATTATCCAAAGAGT-3′ (*Xho*I site (underlined letters) and additional bases are indicated by lowercase letters); *R-Ec*^{icdp}, 5′-CCCTTCTTCAAAACTTACTTTTTCTGCCATTCACCTCTCCTTCGAGCGCTACTGGTTTGC-3′, which contains the promoter sequence of *E. coli icd* gene. The *S. mutans citC* gene was amplified with the following primers: *S-Sm*^{icd}, 5′-GCAAACCAGTAGCG CTCGAAGGAGAGGTGAATGGCAGAAAAAGTAAGTTTTGAAGAAGGG-3′; *R-Sm*^{icd}, 5′-tatattctctgcagCTAGTGGTGGTGGTGGTGGTGTAAATAAGTCAATAGAAC-3′ (*Pst*I site (underlined letters) and additional bases are indicated by lowercase letters) using plasmid pKM49 [31] as template. The 3′ end of *R-Ec*^{icdp} and the 5′ end of *S-Sm*^{icd} were designed to be reverse and complementary to each other so that the two PCR products can be fused together by overlap extension using *S-Ec*^{icdp} and *R-Sm*^{icd} as primers. The resulting 2.0-kb PCR product containing *S. mutans citC* gene preceded by the promoter of *E. coli icd* gene was then ligated into *Xho*I- and *Pst*I-digested pSP72 (Promega) to create pWT.

Site-directed mutagenesis

All mutants (S102T, S102G, S102A, S102Y, S102D and S102E) were constructed by site-directed mutagenesis from pWT. The synthetic oligonucleotide primers are shown in Table 1. The mutations were introduced by sequential steps of PCR. In the first round, two reactions (I and II) were performed with the following primers: *S-Ec*^{icdp} and one of the antisense primers containing the desired mutation (reaction I); one of the sense primers containing the desired mutation and *R-Sm*^{icd} (reaction II). The purified two overlapping fragments were used as templates in the final amplification step with primers *S-Ec*^{icdp} and *R-Sm*^{icd}. All the final PCR products were cloned into pSP72 to obtain plasmids pS102T, pS102G, pS102A, pS102Y, pS102D and

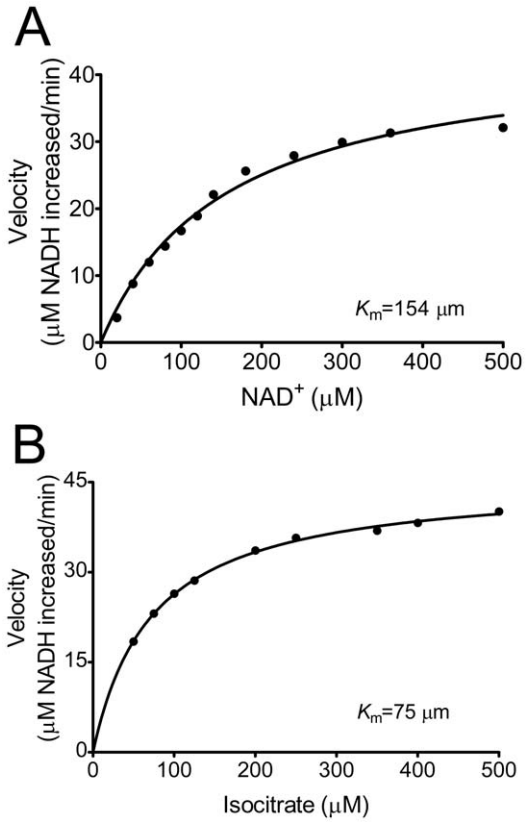

Figure 3. Kinetic analysis of the recombinant SmIDH. The kinetic parameters of the recombinant SmIDH were determined by measuring its enzyme activity at various isocitrate or NAD^+ concentrations with the other substrate at saturating concentrations. Enzymatic activity was assessed by monitoring the increase of NADH. The SmIDH K_m for NAD^+ (A) and isocitrate (B) were calculated as 154 μM and 75 μM, respectively, by averaging values from triplicate experiments.
doi:10.1371/journal.pone.0058918.g003

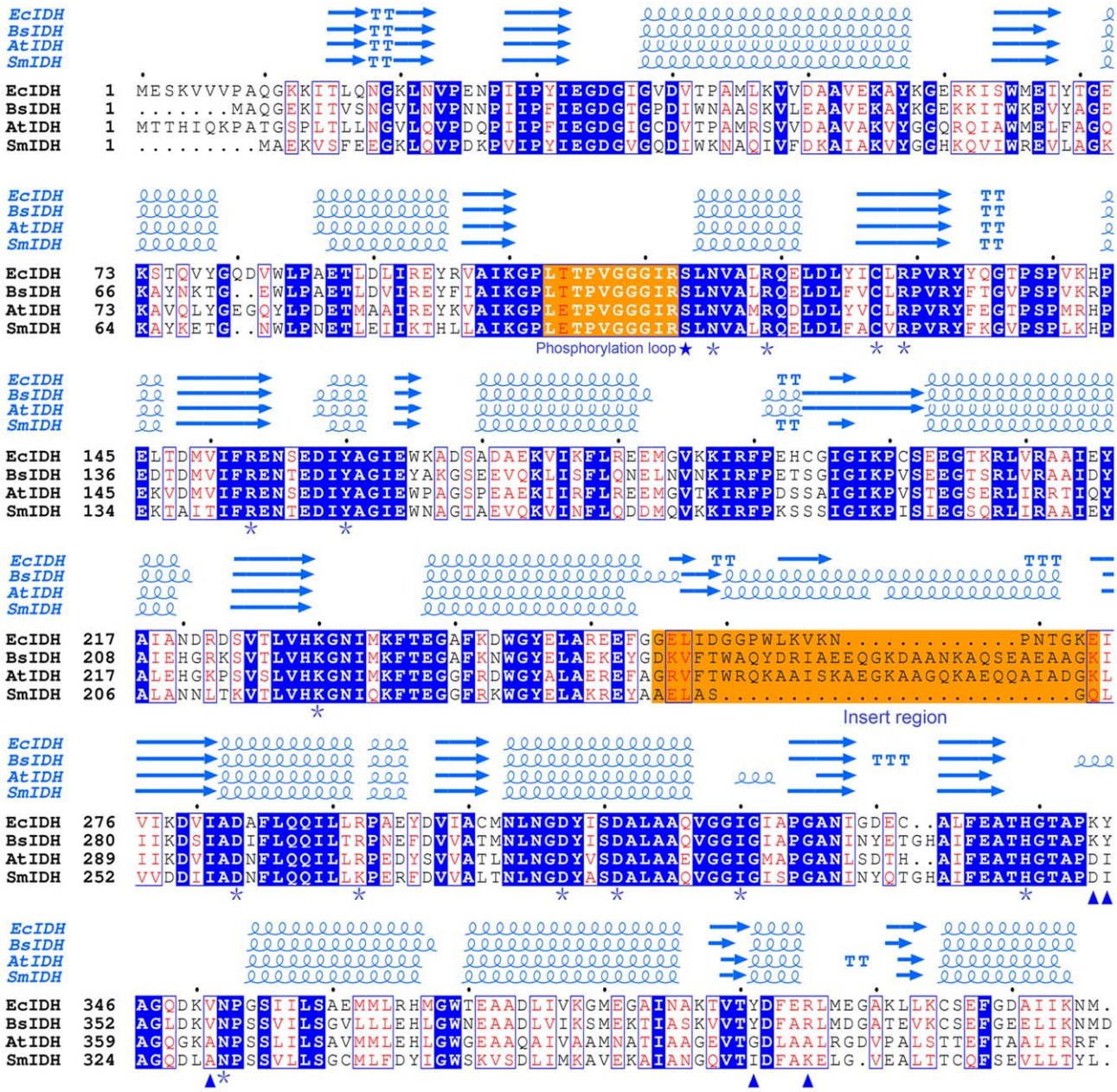

Figure 4. Structure-based protein sequence alignment of SmIDH with other dimeric IDHs. High-resolution crystal structures of *E. coli* NADP-IDH (EcIDH, 9ICD), *B. subtilis* NADP-IDH (BsIDH, 1HQS) and *A. thiooxidans* NAD-IDH (AtIDH, 2D4V) were downloaded from the PDB database. SmIDH structure was generated using the SWISS-MODEL modeling server, using AtIDH as a template structure. Invariant residues are highlighted by shaded blue boxes and conserved residues by open blue boxes. The conserved residues involved in the cofactor binding (▲) and substrate binding (*) are indicated. The phosphorylation site was represented by ★. The phosphorylation loop and the insert region were highlighted by shaded orange boxes. The figure was made with ESPript 2.2 [36].
doi:10.1371/journal.pone.0058918.g004

pS102E. All mutated genes were confirmed by sequencing in both directions.

Protein expression and purification

All recombinant plasmids were transformed into *E. coli* strain *Δicd::kan*^{r}, respectively. The resulting strains were grown overnight at 37°C in LB medium with 100 μg/ml ampicillin, and then inoculated (1:50) into 500 ml of MD medium with the same antibiotic and grown for two days. The cells were harvested by centrifugation, resuspended in wash buffer (10 mM KH_2PO_4 (pH 7.7), 500 mM NaCl, 2 mM $MgCl_2$ and 2 mM β-mercaptoethanol) and disrupted by sonication. Then, cell debris was removed by centrifugation at 11,000 rpm for 10 min. The 6His-tagged wild-type SmIDH and its mutated enzymes were purified using BD TALON Metal Affinity Resin (Clontech, LaJolla, CA, USA) according to the manufacturer's instructions.

Enzyme purity and western blotting

Enzyme purity was determined by SDS-PAGE. For western blotting analysis, SDS-PAGE gels were transferred to nitrocellu-

Table 2. Effects of metal ions on the activity of recombinant SmIDH [a].

Metal ions	Relative activity (%)
None	0
K^+	15±1.7
Na^+	23±2.1
Mn^{2+}	100±0.5
Mg^{2+}	84±2.3
Co^{2+}	7±0.3
Cu^{2+}	1±0.1
Ca^{2+}	0
Zn^{2+}	0
Ni^{2+}	0
K^++Mn^{2+}	108±5.8
Na^++Mn^{2+}	101±4.9
Mg^{2+}+Mn^{2+}	84±2.0
Co^{2+}+Mn^{2+}	11±1.2
Cu^{2+}+Mn^{2+}	12±1.4
Ca^{2+}+Mn^{2+}	81±3.6
Zn^{2+}+Mn^{2+}	2±0.7
Ni^{2+}+Mn^{2+}	1±0.3

[a]The values indicate the means of at least three independent measurements.
doi:10.1371/journal.pone.0058918.t002

lose membranes by electroblotting and blocked for 1 h at room temperature in TBS-T (50 mM Tris-HCl pH 7.5, 150 mM NaCl, 0.2% Tween-20) containing 5% nonfat milk and then washed with TBS-T for three times. His-tag polyclonal antibody (Cell Signaling Technology Inc., Beverly, MA, USA) was applied to the blots for 1 h at room temperature. After three 10-min washes with TBS-T, the blots were incubated for 1 h with alkaline phosphatase conjugated anti-rabbit IgG (Promega, Madison, WI, USA). The blots were washed three times in TBS-T, and bound conjugate was revealed by incubation with the alkaline phosphatase substrate. The chemiluminescence signal corresponding to the specific antibody-antigen reaction was visualized by exposing the blots to X-ray film for 15 minutes in the dark room.

Gel filtration chromatography

The molecular mass of SmIDH was estimated by gel filtration chromatography on a HiLoad^{TM} 10/300 Superdex 200 column (Amersham Biosciences), equilibrated with 0.05 M potassium phosphate buffer (pH 7.0) containing 0.15 M NaCl and 0.01% NaN_3. Protein standards for calibrating gels were Ovalbumin (45 kDa), Conalbumin (75 kDa), Aldolase (158 kDa), Ferritin (440 kDa) and Thyroglobulin (669 kDa).

Circular dichroism spectroscopy of the wild-type and mutant enzymes

Circular dichroism (CD) spectroscopy was conducted using a Jasco model J-810 spectropolarimeter. The ellipticity measurements as a function of wavelength were performed as described previously [32]. Purified protein samples (0.3 mg/ml) were prepared in 50 mM sodium phosphate and 60 mM NaCl (pH 7.5). The ellipticity (θ) was obtained by averaging 3 scans of the enzyme solution between 200 and 260 nm at 0.5 nm increments. The mean molar ellipticity, $[\theta]$ (deg cm^2 dmole^{-1}), was calculated from $[\theta] = \theta/10nCl$, where θ is the measured ellipticity (millidegrees), C is the molar concentration of protein, l is the cell path length in centimeters (0.1 cm), and n is the number of residues per subunit of enzyme (399 for SmIDH and the mutants).

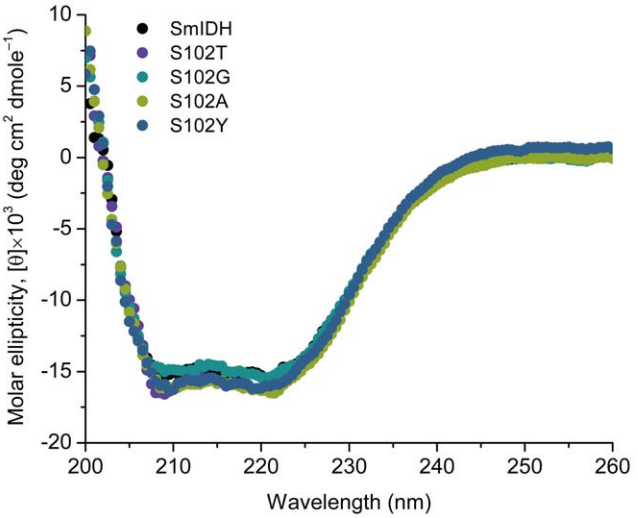

Figure 5. Circular diochroism (CD) spectra of the wild-type SmIDH and four mutants, S102T, S102G, S102A and S102Y. The CD was measured and the molar ellipticity was calculated as described in Materials and methods.
doi:10.1371/journal.pone.0058918.g005

Enzyme assays and kinetic studies

The enzyme activity was assayed by a modification of the method described previously [33]. Reaction mixtures were incubated at 37°C in 1 ml volume containing 35 mM Tris-HCl buffer (pH 7.5), 3.5 mM MnCl2, 2.5 mM DL-isocitrate, 0.5 mM NAD^+ or 5 mM $NADP^+$. The increase in NADPH or NADH was monitored at 340 nm with a thermostated Cary 300 UV-Vis spectrophotometer (Varian, CA, USA) using a molar extinction coefficient of 6220 M^{-1} cm^{-1}. One unit (U) of activity was defined as 1 μmol NADPH or NADH formed per minute. The apparent kinetic parameters were calculated by nonlinear regression using the program Prism 5.0 (Prism, GraphPad Software, CA, USA). All kinetic parameters were obtained from at least three measurements. The concentrations of the purified enzymes were estimated by absorbance measurements at 280 nm, using an extinction coefficient ($\varepsilon_{280} = 51{,}255$) calculated by the method of Pace et al. [34].

Effects of pH and temperature

The enzyme was assayed in 35 mM Tris-HCl buffer between pH 7.2 and 9.2. The optimum temperature was determined by the standard activity assay at different temperatures from 25°C to 55°C. To estimate thermal stability, enzymes were incubated for 20 min between 25 and 55°C in a water bath. Aliquots were withdrawn at periodic intervals, cooled in an ice bath and assayed as described above.

Metal ions effect

The effects of different metal ions (2 mM $MnCl_2$, 2 mM $MgCl_2$, 2 mM $CaCl_2$, 2 mM $CoCl_2$, 2 mM $CuCl_2$, 2 mM $ZnSO_4$, 2 mM $NiSO_4$, 2 mM NaCl and 2 mM KCl) on SmIDH activities were determined using the standard assay procedures.

Table 3. Kinetic parameters of SmIDH and its mutants for isocitrate and NAD^+.

Enzyme	Isocitrate			NAD^+		
	K_m (μM)	k_{cat} (s^{-1})	k_{cat}/K_m (μM^{-1} s^{-1})	K_m (μM)	k_{cat} (s^{-1})	k_{cat}/K_m (μM^{-1} s^{-1})
SmIDH	75	124	1.65	154	56	0.36
S102T	150	25	0.17	350	59	0.17
S102G	143	4	0.028	295	9.1	0.03
S102A	148	3.3	0.022	246	3	0.01
S102Y	385	1.5	0.004	1560	3.5	0.002

doi:10.1371/journal.pone.0058918.t003

Structure-based amino acid sequence alignment

X-ray structures of *E. coli* NADP-IDH (EcIDH, PDB code 9ICD), *Bacillus subtilis* NADP-IDH (BsIDH, 1HQS) and *Acidithiobacillus thiooxidans* NAD-IDH (AtIDH, 2D4V) were downloaded from the PDB database (http://www.rcsb.org/pdb/). The homology model of SmIDH was generated by SWISS-MODEL server (http://swissmodel.expasy.org). Structure-based amino acid sequence alignment was conducted with ClustalX program (ftp://ftp.ebi.ac.uk/pub/software/clustalw2) and ESPript 2.2 web tool (http://espript.ibcp.fr/ESPript/ESPript/) [35,36].

Results and Discussion

Expression and purification of recombinant SmIDH

As the recombinant SmIDH can not be produced in *E. coli* under the control of the *lac* promoter, a unique IDH expression method was applied in this study. The promoter sequence of *E. coli icd* gene was firstly fused to the N-terminus of *S. mutans citC* gene and then subcloned together into the vector pSP72, creating pWT. The recombinant plasmid pWT was transformed into the glutamate auxotrophic *E. coli* strain *Δicd::kan*^{r} (*icd*-defective strain). The expression of *S. mutans citC* gene was examined by evaluating the strain growth on minimal medium containing glucose as the sole carbon source without glutamate. The transformants that grew well on the minimal medium were isolated, indicating that *S. mutans citC* gene can be expressed normally and function well by restoring the growth of *E. coli* strain *Δicd::kan*^{r}.

SmIDH was produced as a 6-histidine fusion protein that had a calculated molecular mass of 43 kDa. A single band at around 43 kDa was visible on the SDS-PAGE gel (Figure 1A), which was confirmed by Western blotting using anti-His antibody (Figure 1B).

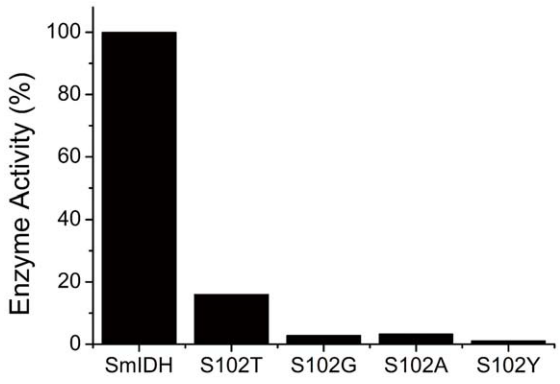

Figure 6. The residual activities of the four Ser102 mutants as compared to the wild-type SmIDH.
doi:10.1371/journal.pone.0058918.g006

Gel filtration chromatography was performed to determinate the oligomerization status of SmIDH in solution. The native molecular mass of SmIDH estimated by gel filtration was 70 kDa (Figure 1C), suggesting a homodimeric structure similar to *E. coli* IDH, *B. subtilis* IDH and *A. thiooxidans* IDH [8,26,37].

Characterization of the enzymatic properties of SmIDH

The effects of pH on SmIDH activity were performed in the pH range of 7.2–9.2. SmIDH was found to have an optimal pH range of 7.5–8.5, with the optimal pH at 7.8 (Figure 2A), lower than that of the NAD^+-IDHs from *A. thiooxidans* (pH 8.5) [2] and *Hydrogenobacter thermophilus* (pH 10.5) [38]. When compared with the broad optimum pH range of $NADP^+$-IDHs from other sources, such as *Streptomyces lividans* (pH 8.5–10.0) [39], *Fomitopsis palustris* (pH 8.0–10.0) [40] and *Aspergillus niger* (pH 6.0–8.0) [41], it was narrower for SmIDH, suggesting that SmIDH was sensitive to pH changes.

SmIDH had a temperature optimum for activity at 40–53°C and its maximum activity was observed at 45°C (Figure 2B). Although this mesophilic enzyme is stable at room temperature, 50% loss of activity and almost complete inactivation were observed after incubation at 43°C and 50°C for 20 min, respectively (Figure 2C). This data was quite different from some known NAD^+-IDHs while most of them were found to be thermostable, such as *A. thiooxidans* IDH (stable up to 55°C) [2], *Methylococcus capsulatus* IDH (optimum for activity at 55–60°C) [4], *H. thermophilus* IDH (half-inactivation at 88.7°C) [3] and most distinguished *P. furiosus* IDH (with a melting temperature of 103.7°C) [5]. The significant difference in thermostability among NAD^+-IDHs could be the temperature adaptation of enzymes to their niches.

Kinetic studies revealed that the apparent K_m of SmIDH displayed for NAD^+ and isocitrate was 154 μM and 75 μM, respectively (Figure 3). The K_m value of SmIDH for NAD^+ was higher than those determined for *P. furiosus* IDH (68.3 μM) and *M. capsulatusbut* IDH (122 μM), but lower than that observed for NAD^+-IDHs from *A. thiooxidans* (180 μM), *Streptococcus suis* (233 μM), *Zymomonas mobilis* (312 μM) and *H. thermophilus* IDH (357 μM) [2–7]. SmIDH was completely NAD^+ dependent as shown and no enzyme activity was observed for SmIDH when NAD^+ was substituted by $NADP^+$ in concentrations up to 5 mM. The cofactor discrimination of IDH was determined by only a few amino acids [42]. In some $NADP^+$-IDHs, such as EcIDH and BsIDH, $Lys^{344/350}$ and $Tyr^{345/351}$ are the major $NADP^+$-specificity determinants (Figure 4), which are substituted by the conserved Asp and Ile in all known NAD^+-IDHs such as $Asp^{322/357}$ and $Ile^{323/358}$ in SmIDH and AtIDH (Figure 4). These major specificity determinants can be used as reliable landmarks to predict the coenzyme specificity of new IDHs.

The effects of nine different metal ions on SmIDH activity were examined (Table 2). SmIDH activity was entirely dependent on the presence of a divalent cation, and Mn^{2+} was found to be the most favored one although Mg^{2+} can partially replace it. In the presence of Mn^{2+}, the addition of 2 mM Co^{2+}, Cu^{2+}, Zn^{2+} and Ni^{2+} reduced SmIDH activity to about 11%, 12%, 2% and 1% of control value, respectively (Table 2). However, the dramatic inhibition of Ca^{2+} on SmIDH activity was not observed in our study. This was quite different from some reports on $NADP^+$-IDHs, such as *E. coli* IDH and *S. lividans* IDH, that Ca^{2+} may reduce the activity at a large scale [39,43]. Neither Na^+ nor K^+ affected SmIDH activity in the presence of Mn^{2+}.

Performances of Ser102 mutants

IDH is the first bacterial enzyme shown to be regulated by phosphorylation/dephosphorylation [44]. The modulation of IDH activity enables *E. coli* to make rapid shifts between TCA and glyoxalate bypass pathways, whereas the phosphorylation state of IDH determines its activity [45–47]. Phosphorylation on a serine residue of EcIDH by IDH K/P inactivates the enzyme by preventing $NADP^+$ binding, and dephosphorylation reactivates it [44,46,48]. Although an analogous serine has been found to be highly conserved in all known NAD^+-IDHs, which is corresponding to the phosphorylation site of Ser113 in EcIDH, there were no reports on evaluating the role of the analogous serine in the regulatory mechanism of NAD^+-IDH activity yet.

A putative phosphorylation site Ser102 was present in the NAD^+-dependent SmIDH. Given the highly structural similarity of SmIDH to EcIDH (Figure 4), the same phosphorylation regulatory mechanism might be used by SmIDH, even though phosphorylation *in vivo* has not been found yet. In this study, we mimicked the phosphorylation state of Ser102 by mutating Ser102 to Asp or Glu (S102D or S102E). The *icd*-defective strain *E. coli* Δ*icd*::*kan*^{r} harboring the recombinant plasmid pS102D or pS102E did not show any growth on MD medium without glutamate, indicating that the mutations of S102D or S102E caused total loss of SmIDH activity. Similar results were reported by Thorsness et al. [24] and Matsuno et al. [31], and they found that both EcIDH and BsIDH were nearly abolished by replacing Ser with Asp in the active site. Given the possibility that a small amount of activity can be retained by S102D and S102E mutants, as observed in S113D and S113E mutants of EcIDH in the previous studies [22,23,25,49], the residual activities of the mutants were so low that the *icd*-defective *E. coli* was not able to survive on MD plates without glutamate.

Phylogenetic analysis reveals that NAD^+ use by IDH is an ancestral phenotype and $NADP^+$ use by prokaryotic IDH arose on or about the time that eukaryotic mitochondria first appeared, some 3.5 billion years ago. The switch of the coenzyme specificity of prokaryotic IDH from NAD^+ to $NADP^+$ is an ancient adaptation to anabolic demand for NADPH during growth on acetate [1]. The anaerobic, Gram-positive bacterium *S. mutans* has an IDH with ancient NAD^+-dependency, suggesting that *S. mutans* might be an ancient prokaryote and not be selected by poor carbon sources (i.e. two carbon compounds) through its evolutionary history. Mimicking phosphorylation by replacing Ser102 with Asp or Glu inactivates SmIDH, implying that Ser102 is a potential phosphorylation site and the ancient NAD-dependent IDHs might be the underlying origin of "phosphorylation mechanism" used by their bacterial NADP-dependent homologs.

The effects of amino acids with different size of side chains, such as Thr, Gly, Ala and Tyr, at the site 102 were also investigated. *E. coli* Δ*icd*::*kan*^{r} strains containing pS102T, pS102G, pS102A and pS102Y showed different growth performances in minimal media, respectively, and the four mutant enzymes were then purified to homogeneity. CD spectra of the wild-type and mutant SmIDH were measured to evaluate whether there is any change in secondary structure of these mutant enzymes. The CD spectra of S102T, S102G, S102A, and S102Y mutants are very similar to that of the wild-type enzyme (Figure 5), suggesting that the mutations did not cause any appreciable conformational change. Four mutants decreased the affinity to isocitrate with 2- to 5-fold K_m values of the wild-type enzyme. Consequently, the catalytic efficiency (k_{cat}/K_m) of them was remarkably reduced about 10- to 412-fold, and S102T, S102G, S102A and S102Y only retained 16.0%, 2.8%, 3.3% and 1.1% of the original activity, respectively (Figure 6). In S102T mutant enzyme, the Thr residue has a γ-hydroxyl side chain as Ser that can bind isocitrate by a hydrogen-bond and thus making S102T retain a relative high activity. The activities of S102Y, S102G and S102A were mainly depended on the size of the side chain of replaced residues, as the bulky side chain in the active site is sterically unfavorable for isocitrate and cofactor binding [22,25]. For example, the replaced Tyr in S102Y, an amino acid with large side chain, caused almost 99% activity loss of SmIDH (Figure 6). The dramatic loss of S102Y activity was mainly caused by its decreased substrate- and cofactor-binding abilities. As shown in Table 3, the K_m values for isocitrate and NAD^+ of S102Y were increased 5.1-fold (from 75 to 385 μM) and 10.1-fold (from 154 to 1560 μM), respectively.

Taken together, six mutations were introduced into SmIDH at Ser102 respectively. Two mutant enzymes lost the activity, and the other four mutants significantly decreased the activity. Apparently, SmIDH activity is sensitive to the substitution at position 102, the conserved Ser102 plays important role in substrate binding and is required for maintaining the proper structure of the active site and responsible for the enzyme function. It implies that SmIDH may have the similar quaternary structure and catalytic mechanism to the well-known NADP-IDHs, such as EcIDH and BsIDH. In addition, the completely conservation of the so-called "phosphorylation loop" and the missing of the "insert-region" (Figure 4), which restricts the access of *E. coli* IDH K/P to the phosphorylation site in BsIDH [26], suggest that SmIDH could be a better substrate for *E. coli* IDH K/P than BsIDH.

Acknowledgments

We are very grateful to professor Antony M. Dean (University of Minnesota, USA) for providing the *icd*-defective *E. coli* strain. We are also very grateful to professor Yunyu Shi (University of Science and Technology of China, China) for her helpful assistance of circular dichroism experiments.

Author Contributions

Conceived and designed the experiments: PW GZ. Performed the experiments: PW PS MJ. Analyzed the data: PW GZ. Contributed reagents/materials/analysis tools: PW PS MJ. Wrote the paper: PW GZ.

References

1. Zhu G, Golding GB, Dean AM (2005) The selective cause of an ancient adaptation. Science 307: 1279–1282.
2. Inoue H, Tamura T, Ehara N, Nishito A, Nakayama Y, et al. (2002) Biochemical and molecular characterization of the NAD^+-dependent isocitrate dehydrogenase from the chemolithotroph *Acidithiobacillus thiooxidans*. FEMS Microbiol Lett 214: 127–132.

3. Aoshima M, Ishii M, Igarashi Y (2004) A novel biotin protein required for reductive carboxylation of 2-oxoglutarate by isocitrate dehydrogenase in *Hydrogenobacter thermophilus* TK-6. Mol. Microbiol 51: 791–798.
4. Stokke R, Madern D, Fedøy AE, Karlsen S, Birkeland NK, et al. (2007) Biochemical characterization of isocitrate dehydrogenase from *Methylococcus capsulatus* reveals a unique NAD-dependent homotetrameric enzyme. Arch Microbiol 187: 361–370.
5. Steen IH, Madern D, Karlström M, Lien T, Ladenstein R, et al. (2001) Comparison of isocitrate dehydrogenase from three hyperthermophiles reveals differences in thermostability, cofactor specificity, oligomeric state, and phylogenetic affiliation. J Biol Chem 276: 43924–43931.
6. Wang P, Jin MM, Su RR, Song P, Wang M, et al. (2011) Enzymatic characterization of isocitrate dehydrogenase from an emerging zoonotic pathogen *Streptococcus suis*. Biochimie 93: 1470–1475.
7. Wang P, Jin MM, Zhu GP (2012) Biochemical and molecular characterization of NAD^+-dependent isocitrate dehydrogenase from the ethanologenic bacterium *Zymomonas mobilis*. FEMS Microbiol Lett 327: 134–141.
8. Imada K, Tamura T, Takenaka R, Kobayashi I, Namba K, et al. (2008) Structure and quantum chemical analysis of NAD^+-dependent isocitrate dehydrogenase: Hydride transfer and co-factor specificity. Proteins: Struct Funct Bioinf 70: 63–71.
9. Taylor AB, Hu G, Hart PJ, McAlister-Henn L (2008) Allosteric motions in structures of yeast NAD^+-specific isocitrate dehydrogenase. J Biol Chem 283: 10872–10880.
10. Ceccarelli C, Grodsky NB, Ariyaratne N, Colman RF, Bahnson BJ (2002) Crystal structure of porcine mitochondrial $NADP^+$-dependent isocitrate dehydrogenase complexed with Mn^{2+} and isocitrate. Insights into the enzyme mechanism. J Biol Chem 277: 43454–43462.
11. Xu X, Zhao J, Xu Z, Peng B, Huang Q, et al. (2004) Structures of human cytosolic NADP-dependent isocitrate dehydrogenase reveal a novel self-regulatory mechanism of activity. J Biol Chem 279: 33946–33957.
12. Jo SH, Son MK, Koh HJ, Lee SM, Song IH, et al. (2001) Control of mitochondrial redox balance and cellular defense against oxidative damage by mitochondrial $NADP^+$-dependent isocitrate dehydrogenase. J Biol Chem 276: 16168–16176.
13. Kim SY, Park JW (2003) Cellular defense against singlet oxygen-induced oxidative damage by cytosolic $NADP^+$-dependent isocitrate dehydrogenase. Free Radic Res 37: 309–316.
14. Kim HJ, Kang BS, Park JW (2005) Cellular defense against heat shock-induced oxidative damage by mitochondrial $NADP^+$-dependent isocitrate dehydrogenase. Free Radic Res 39: 441–448.
15. Lee SM, Koh HJ, Park DC, Song BJ, Huh TL, et al. (2002) Cytosolic $NADP^+$-dependent isocitrate dehydrogenase status modulates oxidative damage to cells. Free Radic Biol Med 32: 1185–1196.
16. Yan H, Parsons DW, Jin G, McLendon R, Rasheed BA, et al. (2009) *IDH1* and *IDH2* mutations in gliomas. N Engl J Med 360: 765–773.
17. Gross S, Cairns RA, Minden MD, Driggers EM, Bittinger MA, et al. (2009) Cancer-associated metabolite 2-hydroxyglutarate accumulates in acute myelogenous leukemia with isocitrate dehydrogenase 1 and 2 mutations. J Exp Med 207: 339–344.
18. Krell D, Assoku M, Galloway M, Mulholland P, Tomlinson I, et al. (2011) Screen for *IDH1*, *IDH2*, *IDH3*, *D2HGDH* and *L2HGDH* mutations in glioblastoma. PLoS ONE 6(5): e19868.
19. Dang L, White DW, Gross S, Bennett BD, Bittinger MA, et al. (2009) Cancer-associated IDH1 mutations produce 2-hydroxyglutarate. Nature 462: 739–744.
20. Jin G, Reitman ZJ, Spasojevic I, Batinic-Haberle I, Yang J, et al. (2011) 2-hydroxyglutarate production, but not dominant negative function, is conferred by glioma-derived $NADP^+$-dependent isocitrate dehydrogenase mutations. PLoS ONE 6(2): e16812.
21. LaPorte DC (1993) The isocitrate dehydrogenase phosphorylation cycle: regulation and enzymology. J Cell Biochem 51: 14–18.
22. Hurley JH, Dean AM, Sohl JL, Koshland DE Jr, Stroud RM (1990) Regulation of an enzyme by phosphorylation at the active site. Science 249: 1012–1016.
23. Dean AM, Lee MH, Koshland DE Jr (1989) Phosphorylation inactivates *Escherichia coli* isocitrate dehydrogenase by preventing isocitrate binding. J Biol Chem 264: 20482–20486.
24. Thorsness PE, Koshland DE Jr (1987) Inactivation of isocitrate dehydrogenase by phosphorylation is mediated by the negative charge of the phosphate. J Biol Chem 262: 10422–10425.
25. Dean AM, Koshland DE Jr (1990) Electrostatic and steric contributions to regulation at the active site of isocitrate dehydrogenase. Science 249: 1044–1046.
26. Singh SK, Matsuno K, LaPorte DC, Banaszak LJ (2001) Crystal structure of *Bacillus subtilis* isocitrate dehydrogenase at 1.55 Å. Insights into the nature of substrate specificity exhibited by *Escherichia coli* isocitrate dehydrogenase kinase/phosphatase. J Biol Chem 276: 26154–26163.
27. Singh SK, Miller SP, Dean A, Banaszak LJ, LaPorte DC (2002) *Bacillus subtilis* isocitrate dehydrogenase. A substrate analogue for *Escherichia coli* isocitrate dehydrogenase kinase/phosphatase. J Biol Chem 277: 7567–7573.
28. Peng Y, Zhong C, Huang W, Ding J (2008) Structural studies of *Saccharomyces cerevesiae* mitochondrial NADP-dependent isocitrate dehydrogenase in different enzymatic states reveal substantial conformational changes during the catalytic reaction. Protein Sci 17: 1542–1554.
29. Chang F, Lemmon C, Lietha D, Eck M, Romer L (2011) Tyrosine phosphorylation of Rac1: a role in regulation of cell spreading. PLoS ONE 6(12): e28587.
30. Zaremba-Czogalla M, Piekarowicz K, Wachowicz K, Kozioł K, Dubińska-Magiera M, et al. (2012) The different function of single phosphorylation sites of *Drosophila melanogaster* lamin Dm and lamin C. PLoS ONE 7(2): e32649.
31. Matsuno K, Blais T, Serio AW, Conway T, Henkin TM, et al. (1999) Metabolic imbalance and sporulation in an isocitrate dehydrogenase mutant of *Bacillus subtilis*. J Bacteriol 181: 3382–3391.
32. Pace CN, Vajdos F, Fee L, Grimsley G, Gray T (1995) How to measure and predict the molar absorption coefficient of a protein. Protein Sci 4: 2411–2423.
33. Cvitkovitch DG, Gutierrez JA, Bleiweis AS (1997) Role of the citrate pathway in glutamate biosynthesis by *Streptococcus mutans*. J Bacteriol 179: 650–655.
34. Grodsky NB, Soundar S, Colman RF (2000) Evaluation by site-directed mutagenesis of aspartic acid residues in the metal site of pig heart NADP-dependent isocitrate dehydrogenase. Biochemistry 39: 2193–2200.
35. Larkin MA, Blackshields G, Brown NP, Chenna R, McGettigan PA, et al. (2007) Clustal W and Clustal X version 2.0. Bioinformatics 23: 2947–2948.
36. Gouet P, Courcelle E, Stuart DI, Métoz F (1999) ESPript: analysis of multiple sequence alignments in PostScript. Bioinformatics 15: 305–308.
37. Hurley JH, Dean AM, Koshland DE Jr, Stroud RM (1991) Catalytic mechanism of $NADP^+$-dependent isocitrate dehydrogenase: implications from the structures of magnesium-isocitrate and $NADP^+$ complexes. Biochemistry 30: 8671–8678.
38. Aoshima M, Igarashi Y (2008) Nondecarboxylating and decarboxylating isocitrate dehydrogenases: oxalosuccinate reductase as an ancestral form of isocitrate dehydrogenase. J Bacteriol 190: 2050–2055.
39. Zhang B, Wang B, Wang P, Cao Z, Huang E, et al. (2009) Enzymatic characterization of a monomeric isocitrate dehydrogenase from *Streptomyces lividans* TK54. Biochimie 91: 1405–1410.
40. Yoon JJ, Hattori T, Shimada M (2003) Purification and characterization of NADP-linked isocitrate dehydrogenase from the copper-tolerant wood-rotting basidiomycete *Fomitopsis palustris*. Biosci Biotechnol Biochem 67: 114–120.
41. Meixner-Monori B, Kubicek CP, Harrer W, Schreferl G, Rohr M (1986) NADP-specific isocitrate dehydrogenase from the citric acid-accumulating fungus *Aspergillus niger*. Biochem J 236: 549–557.
42. Hurley JH, Chen R, Dean AM (1996) Determinants of cofactor specificity in isocitrate dehydrogenase: structure of an engineered $NADP^+ \rightarrow NAD^+$ specificity reversal mutant. Biochemistry 35: 5670–5678.
43. Stoddard BL, Dean AM, Koshland DE Jr (1993) Structure of isocitrate dehydrogenase with isocitrate, nicotinamide adenine dinucleotide phosphate, and calcium at 2.5-Å resolution: a pseudo-Michaelis ternary complex. Biochemistry 32: 9310–9316.
44. Borthwick AC, Holms WH, Nimmo HG (1984) The phosphorylation of *Escherichia coli* isocitrate dehydrogenase in intact cells. Biochem J 222: 797–804.
45. Walsh K, Koshland DE Jr (1985) Branch point control by the phosphorylation state of isocitrate dehydrogenase. A quantitative examination of fluxes during a regulatory transition. J Biol Chem 260: 8430–8437.
46. McKee JS, Nimmo HG (1989) Evidence for an arginine residue at the coenzyme-binding site of *Escherichia coli* isocitrate dehydrogenase. Biochem J 261: 301–304.
47. LaPorte DC, Walsh K, Koshland DE Jr (1984) The branch point effect. Ultrasensitivity and subsensitivity to metabolic control. J Biol Chem 259: 14068–14075.
48. Hurley JH, Thorsness PE, Ramalingam V, Helmers NH, Koshland DE Jr, et al. (1989) Structure of a bacterial enzyme regulated by phosphorylation, isocitrate dehydrogenase. Proc Natl Acad Sci USA 86: 8635–8639.
49. Chen R, Grobler JA, Hurley JH, Dean AM (1996) Second-site suppression of regulatory phosphorylation in *Escherichia coli* isocitrate dehydrogenase. Protein Sci 5: 287–295.